DOI: 10.17512/znb.2017.1.21

Jozef Melcer[1]

DYNAMIC LOAD ON PAVEMENT - NUMERICAL ANALYSIS

Introduction

The roads are the transport structures subjected to direct dynamic effect of moving vehicles. The knowledge of the real load acting on the roads and vehicle behaviour, the variability in time and frequency composition, is needed for the solution of many engineering tasks as design, fatigue, lifetime, reliability, maintenance, structure development, micro-tremor, etc. [1-5]. The task can be solved by experimental or by numerical way. But the most effective way is the combination of the both mentioned advances. The submitted paper is dedicated to the description of facilities how to obtained the required data by numerical way in time domain. This process includes creation the computing models of vehicles, the computing models of the roads and generation of the road unevenness. The attention must be paid to the numerical solution of equations of motion and valuation of obtained results. It is convenient to utilize the resources of the program system MATLAB [6]. Random road profile must be generated and taken into calculation. The best way is to generate the random road profile by the known power spectral density function [7].

1. Computing model of vehicle

The computing models of vehicles can be created on various levels as 1-dimensional, 2-dimensional or 3-dimensional. Every model has its advantages and disadvantages and under certain assumptions it can be used for the solution of real practical problems.

For the purpose of this contribution the 3-dimensional space computing model of a lorry Tatra 815 was adopted (Fig. 1).

The vehicle computing model is discrete model with 15 degrees of freedom. The 9 mass degrees of freedom correspond to the displacements $r_i(t)$ of the mass objects m_i. The mass-less degree of freedoms correspond to the vertical move-

[1] University of Žilina, Slovak Republic, e-mail: jozef.melcer@fstav.uniza.sk

ments of the contact point of the model with the road surface. The vibration of the mass objects of the model is described by the 9 functions of time $r_i(t)$, ($i = 1 \div 9$). The mass-less degrees of freedom are associated with the tire forces $F_j(t)$, ($j = 10 \div 15$) acting at the contact points.

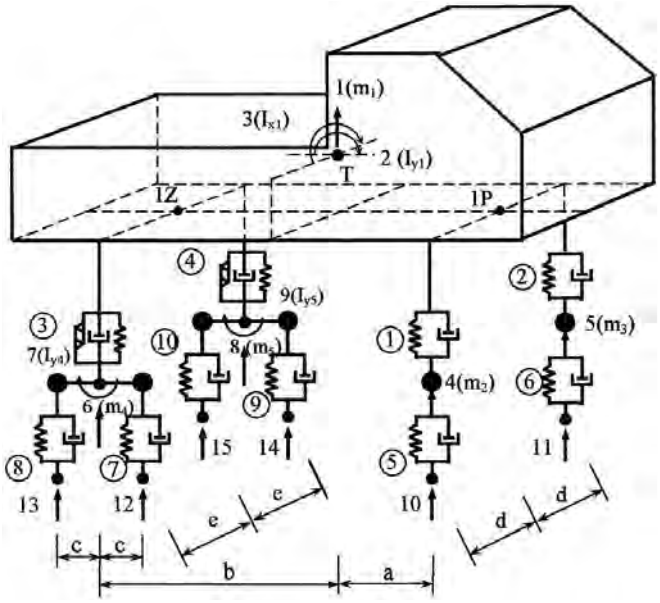

Fig. 1. Space model of the vehicle Tatra 815

In the following text the results of the numerical calculations of natural frequencies and natural modes for computational model of vehicle Tatra T815 are published.

Transposed static matrix

$$[A]^T = \begin{bmatrix} 1 & -a & -d & -1 & 0 & 0 & 0 & 0 & 0 \\ 1 & -a & +d & 0 & -1 & 0 & 0 & 0 & 0 \\ 1 & +b & -e & 0 & 0 & -1 & 0 & 0 & 0 \\ 1 & +b & +e & 0 & 0 & 0 & 0 & -1 & 0 \\ 0 & 0 & 0 & +1 & 0 & 0 & 0 & 0 & 0 \\ 0 & 0 & 0 & 0 & +1 & 0 & 0 & 0 & 0 \\ 0 & 0 & 0 & 0 & 0 & +1 & -c & 0 & 0 \\ 0 & 0 & 0 & 0 & 0 & +1 & +c & 0 & 0 \\ 0 & 0 & 0 & 0 & 0 & 0 & 0 & +1 & -c \\ 0 & 0 & 0 & 0 & 0 & 0 & 0 & +1 & +c \end{bmatrix}$$

$a = 3.135$ m; $b = 1.075$ m; $c = 0.660$ m; $d = 0.993$ m; $e = 0.973$ m.

Diagonal stiffness matrix of connecting members

$$\{\mathbf{k_i}\}_\mathbf{D} = \{k_1; k_2; k_3; k_4; k_5; k_6; k_7; k_8; k_9; k_{10}\}_\mathrm{D} =$$
$$= \{143716.5;\ 143716.5;\ 761256;\ 761256;\ 1275300;$$
$$1275300;\ 2511360;\ 2511360;\ 2511360;\ 2511360\}_\mathrm{D}\ [\mathrm{N/m}]$$

Diagonal mass matrix

$$\{\mathbf{m}\}_\mathbf{D} = \{m_1; I_{y1}; I_{x1}; m_2; m_3; m_4; I_{y4}; m_5; I_{y5}\}_\mathrm{D} =$$
$$= \{22950.0;\ 62298.0;\ 22950.0;\ 455;\ 455;\ 1070;\ 466;\ 1070;\ 466\}_\mathrm{D}\ [\mathrm{kg},\ \mathrm{kg\cdot m^2}]$$

Natural frequencies

$$\{\mathbf{f}\} = \{f_{(1)}; f_{(2)}; f_{(3)}; f_{(4)}; f_{(5)}; f_{(6)}; f_{(7)}; f_{(8)}; f_{(9)}\} =$$
$$= \{1.13;\ 1.29;\ 1.45;\ 8.89;\ 8.89;\ 10.91;\ 10.91;\ 11.71;\ 11.71\}\ [\mathrm{Hz}]$$

Ortonormal natural modes - modal matrix

$$\mathbf{[R]} = \left[\{R_{(1)}\}\ \{R_{(2)}\}\ \{R_{(3)}\}\ \{R_{(4)}\}\ \{R_{(5)}\}\ \{R_{(6)}\}\ \{R_{(7)}\}\ \{R_{(8)}\}\ \{R_{(9)}\}\right] =$$

$$= \begin{bmatrix}
0.00439795 & 0.00000000 & -0.00491329 & 0.00000000 & 0.00013475 \\
-0.00298267 & 0.00000000 & -0.00266827 & 0.00000000 & -0.00015638 \\
0.00000000 & 0.00659444 & 0.00000000 & 0.00013450 & 0.00000000 \\
0.00141546 & -0.00067743 & 0.00035916 & 0.03314273 & -0.03311749 \\
0.00141546 & 0.00067743 & 0.00035916 & -0.03314273 & -0.03311749 \\
0.00015831 & -0.00085485 & -0.00104018 & -0.00004073 & -0.00001041 \\
0.00000000 & 0.00000000 & 0.00000000 & 0.00000000 & 0.00000000 \\
0.00015831 & 0.00085485 & -0.00104018 & -0.00004073 & -0.00001041 \\
0.00000000 & 0.00000000 & 0.00000000 & 0.00000000 & 0.00000000
\end{bmatrix}$$

$$\begin{bmatrix}
0.00000000 & 0.00000000 & 0.00000000 & 0.00026888 \\
0.00000000 & 0.00000000 & 0.00000000 & 0.00010675 \\
0.00000000 & 0.00000000 & -0.00026123 & 0.00000000 \\
0.00000000 & 0.00000000 & -0.00003569 & 0.00000903 \\
0.00000000 & 0.00000000 & 0.00003569 & 0.00000903 \\
0.00000000 & 0.00000000 & -0.02159993 & -0.02159126 \\
0.04632411 & 0.00000000 & 0.00000000 & 0.00000000 \\
0.00000000 & 0.00000000 & 0.02159993 & -0.02159126 \\
0.00000000 & 0.04632411 & 0.00000000 & 0.00000000
\end{bmatrix}$$

Solution of equations of motion in time domain is realized numerically in the environment of programming system MATLAB. The 4th order Runge-Kutta step-by-step integration method is employed.

2. Road surface unevenness

The rigid pavement with random road profile is assumed for the purpose of numerical solution. The random road profile $u(x)$ is assumed as stationary ergodic function with zero mean value and normal distribution. The properties of the road profile are described by Power Spectral Density function (PSD) in the form

$$S_u(\Omega) = S_u(\Omega_0) \cdot \left(\frac{\Omega}{\Omega_0} \right)^{-k} \tag{1}$$

where Ω in [rad/m] denotes the wave number, $\Omega_0 = 1$ rad/m is the reference wave number and the waviness $k = 2$. According to the international directive ISO 8608 [7], typical road profiles can be grouped into classes from A to H. But on the roads actually come into consideration categories A÷E only. Each class is simply defined by its reference value $S_u(\Omega_0)$ (Fig. 2 and Table 1).

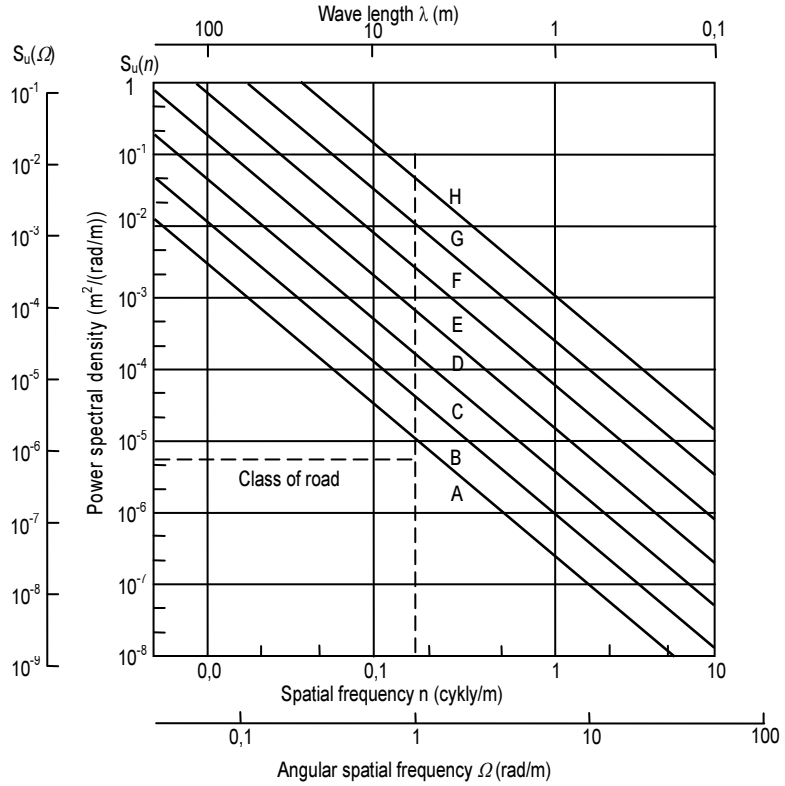

Fig. 2. Power spectral densities of the road profiles by [7]

TABLE 1

Classification of pavements according to road unevenness [6]

Class	$S_u(\Omega_0)$ [m^2/(rad/m)] at Ω_0 = 1 rad/m		
	lower bound	geometric average	upper bound
A	–	$1\cdot10^{-6}$	$2\cdot10^{-6}$
B	$2\cdot10^{-6}$	$4\cdot10^{-6}$	$8\cdot10^{-6}$
C	$8\cdot10^{-6}$	$16\cdot10^{-6}$	$32\cdot10^{-6}$
D	$32\cdot10^{-6}$	$64\cdot10^{-6}$	$128\cdot10^{-6}$
E	$128\cdot10^{-6}$	$256\cdot10^{-6}$	$512\cdot10^{-6}$
F	$512\cdot10^{-6}$	$1024\cdot10^{-6}$	$2084\cdot10^{-6}$
G	$2084\cdot10^{-6}$	$4096\cdot10^{-6}$	$8192\cdot10^{-6}$
H	$8192\cdot10^{-6}$	$16384\cdot10^{-6}$	–

A random profile of a single track can be approximated as

$$u(x) = \sum_{i}^{N} \sqrt{2 \cdot S(\Omega_i) \cdot \Delta\Omega} \cdot \cos(\Omega_i \cdot x + \phi_i) \tag{2}$$

where φ_i is the uniformly distributed phase angle.

In the first step the random road profiles *ul* and *ur* (in left and right tracks) on the basis of known power spectral density for the value $S_u(\Omega_0) = 2\cdot10^{-6}$ m^2/(rad/m), category B, were generated by the Eq. (2) (10 240 samples with the step 0.01 m). The generated road profiles are shown in Figure 3.

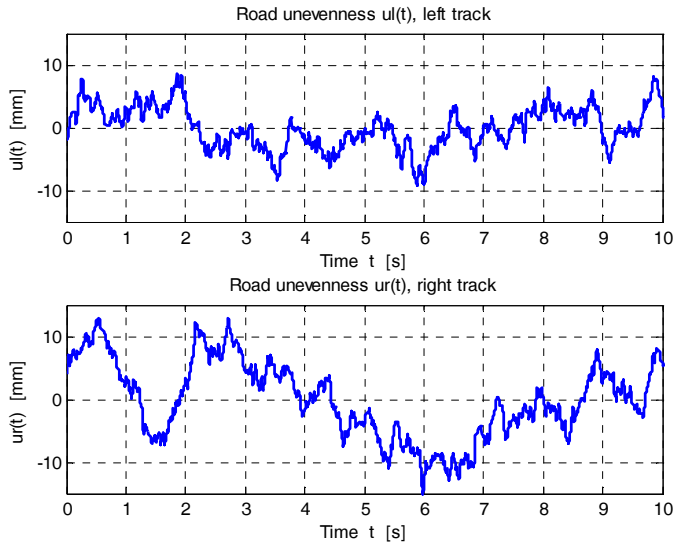

Fig. 3. Random road profile in left and right tracks

The real Power Spectral Densities (PSD) generated back from the numerically obtained left and right road profiles drawn in log-log scale are plotted in Figures 4 and 5.

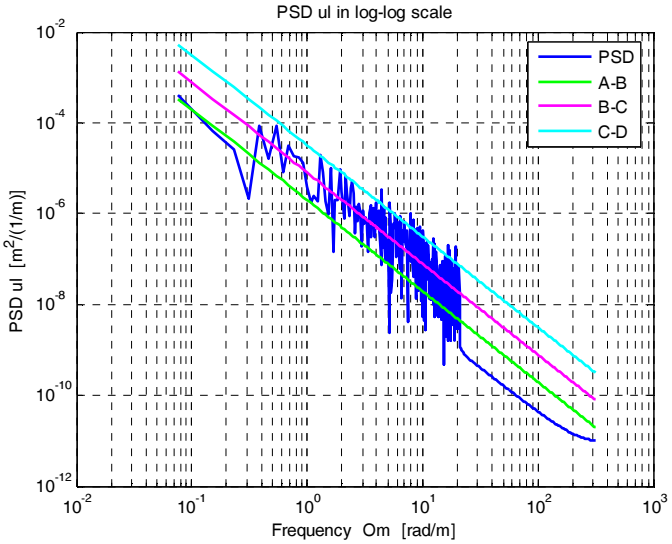

Fig. 4. PSD of left road track

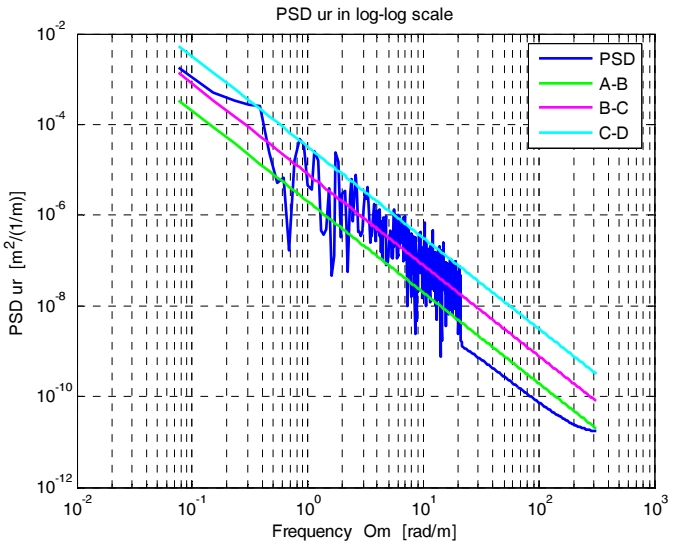

Fig. 5. PSD of right road track

The profiles have $N = 10\ 240$ samples.

The numeral values of road profiles statistical characteristics are put into Table 2.

TABLE 2

Statistical characteristics of road profiles *ul* and *ur*

	ul	*ur*
Mean value $\overline{u}$	0.19e-10 mm	8.04e-10 mm
Arithmetic mean deviation R_a	2.679 mm	5.166 mm
Root mean square average deviation R_q	3.325 mm	6.158 mm
Dispersion σ^2	11.056 mm^2	37.931 mm^2
Effective values - Root mean square value *RMS*	3.325 mm	6.158 mm
Asymmetry coefficient R_{sk}	–0.051	–0.042
Kurtosis R_{ku}	2.796	2.162
Greatest depth of unevenness	–9.281 mm	–15.192 mm
The largest height of unevenness	8.564 mm	12.994 mm
Overall height of the profile	17.845 mm	28.186 mm

The histograms of amplitude distribution are shown in Figures 6 and 7.

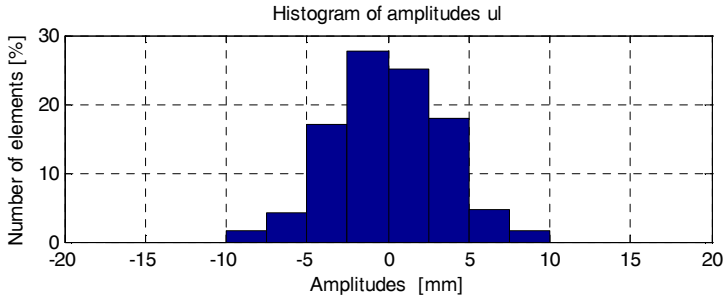

Fig. 6. Histogram of amplitude distribution *ul*

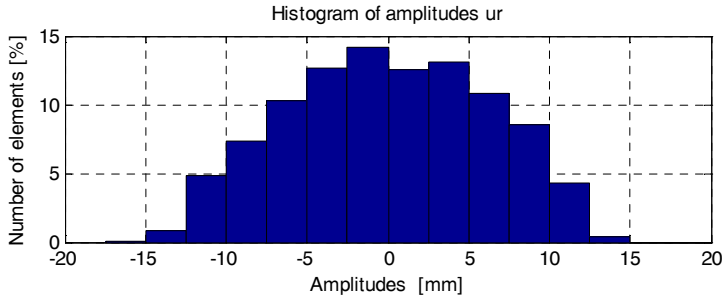

Fig. 7. Histogram of amplitude distribution *ur*

The normalized auto-correlation and normalized cross-correlation functions are plotted in Figures 8-10.

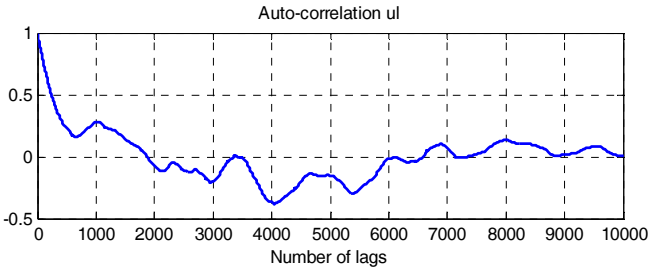

Fig. 8. Normalized auto-correlation function of left road profile *ul*

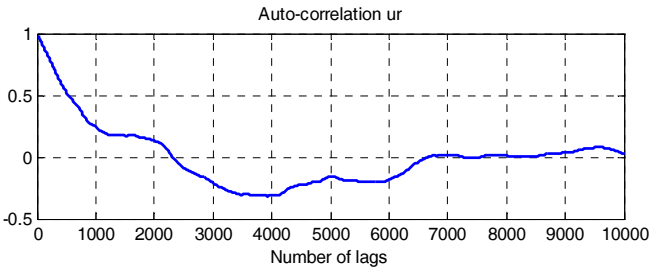

Fig. 9. Normalized auto-correlation function of right road profile *ur*

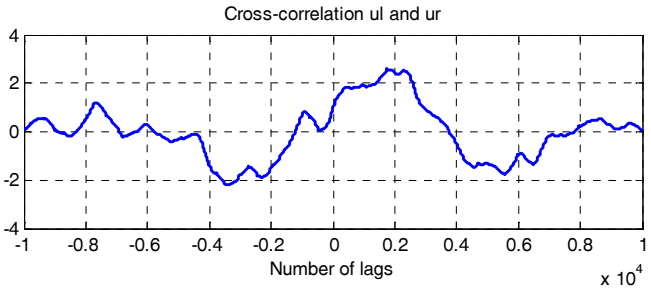

Fig. 10. Normalized cross-correlation function of left and right road profile

3. Vehicle response and dynamic load on pavement

At the second step the vehicle response and dynamic load on pavement were numerically simulated. Numerical solution was carried out in the environment of the program system MATLAB. The 4st order Runge-Kutta step-by-step integration method was used for the solution of equations of motion. As the result of numerical simulation the movement of vehicle along the random road profiles with the speed $V = 36$ km/h was simulated.

Some results of vehicle response are presented in Figures 11-14. The meaning of individual symbols is as follows: r_1 vertical displacement of sprung mass gravity center, r_2, r_3 rotation of sprung mass in longitudinal and transverse directions, r_5, r_4 displacement of left and right front wheel, r_8, r_6 displacement of left and right rear axle, r_9, r_7 rotation of left and right rear axle in longitudinal direction.

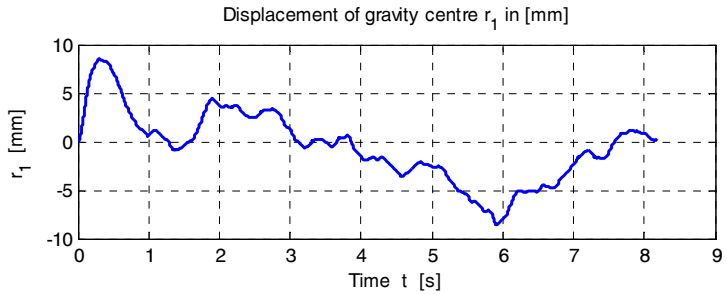

Fig. 11. Response of individual points of vehicle model

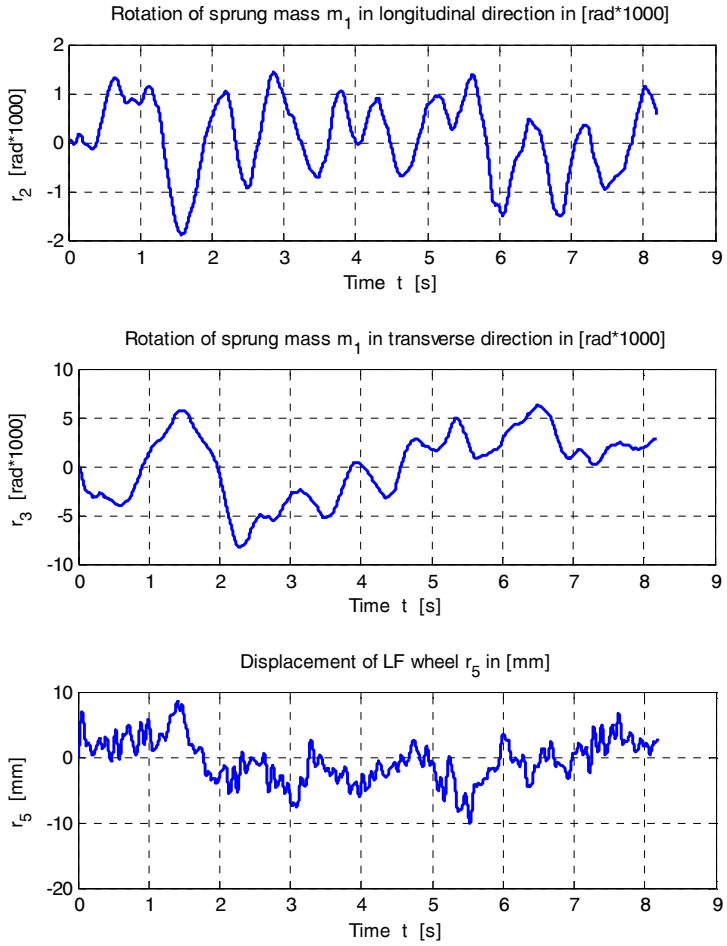

Fig. 12. Response of individual points of vehicle model

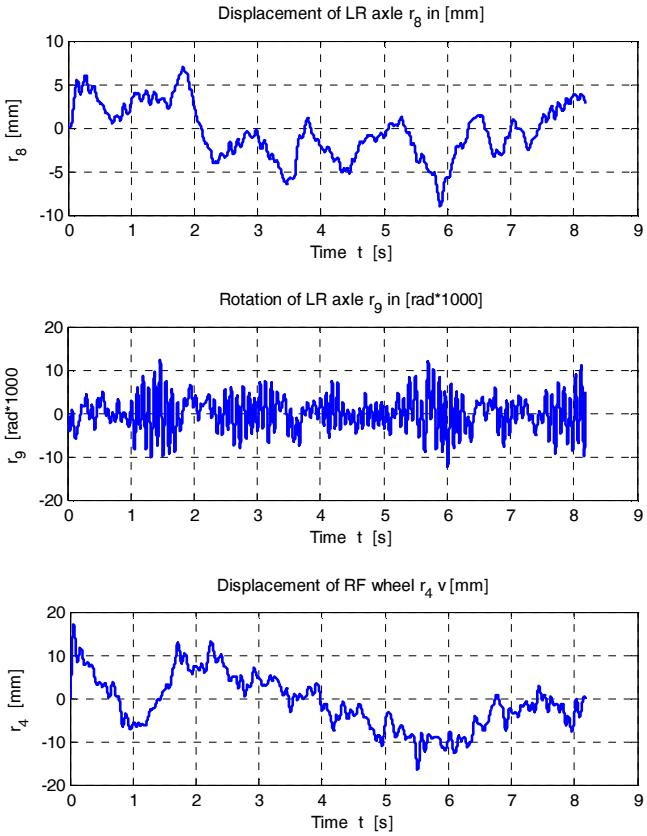

Fig. 13. Response of individual points of vehicle model

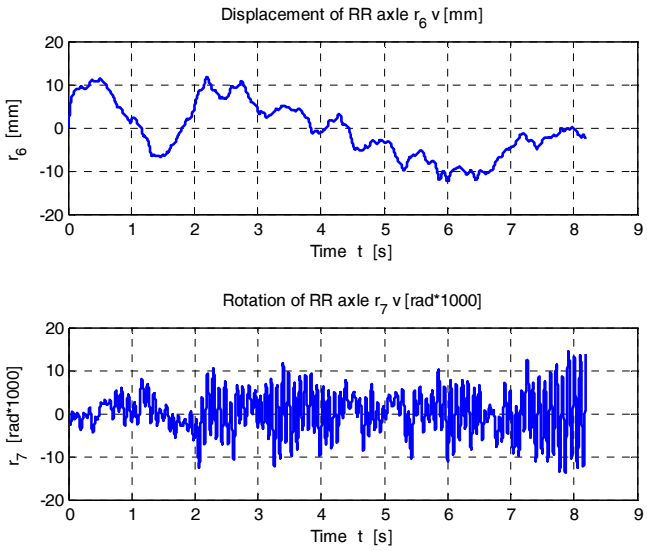

Fig. 14. Response of individual points of vehicle model

In the third step the tire forces $F_j(t)$ under individual wheels of vehicle were calculated. The time histories of tire force under individual wheels on the left and right hand side of vehicle are plotted in Figures 15-18.

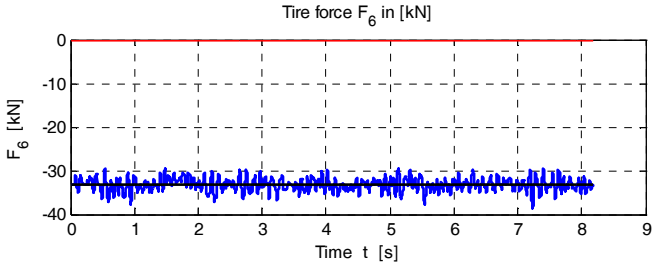

Fig. 15. Tire forces under wheels on the left hand side of vehicle

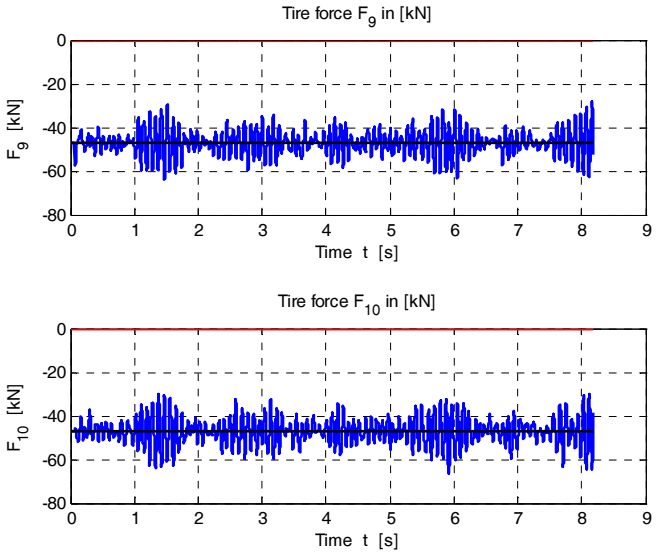

Fig. 16. Tire forces under wheels on the left hand side of vehicle

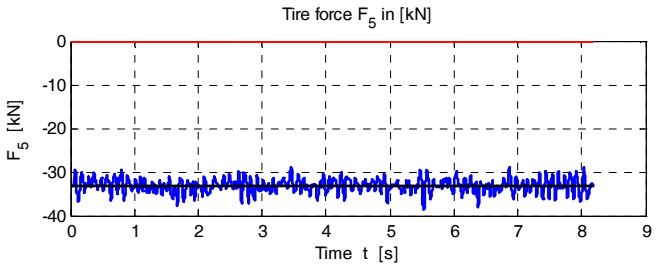

Fig. 17. Tire forces under wheels on the right hand side of vehicle

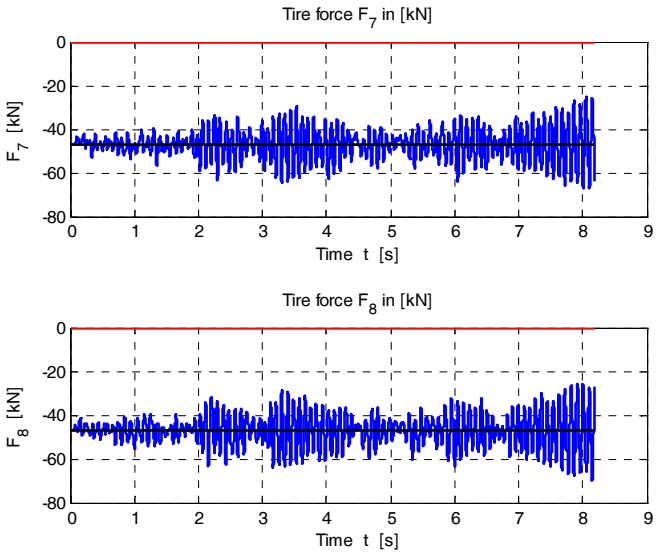

Fig. 18. Tire forces under wheels on the right hand side of vehicle

The road unevenness is the source of kinematical excitation of vehicle. It directly influences the magnitude of tire forces. The influence of the quality of road profile, influence of the range $\Delta ul = ul_{\max} - ul_{\min}$ on the range of tire forces $\Delta F_j = |F_{j,\max}| - |F_{j,\min}|$ for various road categories under wheels on the left hand side of vehicle is shown in Table 3. The influence of the range $\Delta ur = ur_{\max} - ur_{\min}$ on the range of tire forces $\Delta F_j = |F_{j,\max}| - |F_{j,\min}|$ for various road categories under wheels on the right hand side of vehicle is shown in Table 4.

TABLE 3

Influence of the quality of road profile on magnitude of tire forces, wheels on the left side of vehicle

Road category	$S_u(\Omega_0)$ [m^2/(rad/m)]	$\Delta ul = ul_{\max} - ul_{\min}$ [mm]	$\Delta F_6 = \lvert F_{6,\max}\rvert - \lvert F_{6,\min}\rvert$ [kN]	$\Delta F_{10} = \lvert F_{10,\max}\rvert - \lvert F_{10,\min}\rvert$ [kN]
A	$1\cdot10^{-6}$	12.6189	6.5865	25.9036
B	$4\cdot10^{-6}$	25.2379	13.2081	51.8742
C	$16\cdot10^{-6}$	50.4759	26.3335	103.1987
D	$64\cdot10^{-6}$	100.9519	52.8371	207.2494
E	$256\cdot10^{-6}$	201.9038	105.2138	415.1362

At the certain category of road the tire forces are theoretically plus. In reality the contact between the wheel and the road is lost. The wheel will be bounce from the road. On rear wheels of this vehicle computing model such situation occurs at the road category C (Fig. 19). The similar situation on front wheels of this vehicle computing model occurs at the road category E (Fig. 20).

TABLE 4

Influence of the quality of road profile on magnitude of tire forces, wheels on the right side of vehicle

Road category	$S_u(\Omega_0)$ [m^2/(rad/m)]	$\Delta ur = ur_{max} - ur_{min}$ [mm]	$\Delta F_5 = \lvert F_{5,max}\rvert - \lvert F_{5,min}\rvert$ [kN]	$\Delta F_8 = \lvert F_{8,max}\rvert - \lvert F_{8,min}\rvert$ [kN]
A	$1\cdot10^{-6}$	19.9312	6.9857	31.1475
B	$4\cdot10^{-6}$	39.8624	13.9794	62.1344
C	$16\cdot10^{-6}$	79.7248	27.9156	117.6140
D	$64\cdot10^{-6}$	159.4497	55.6924	249.2978
E	$256\cdot10^{-6}$	318.8995	111.6479	498.2201

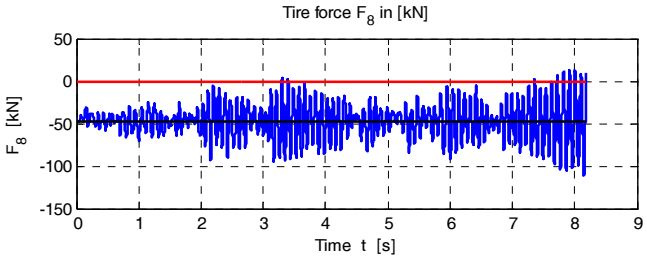

Fig. 19. Tire force under right rear wheel, road category C, $S_u(\Omega_0) = 16\cdot10^{-6}$ m^2/(rad/m)

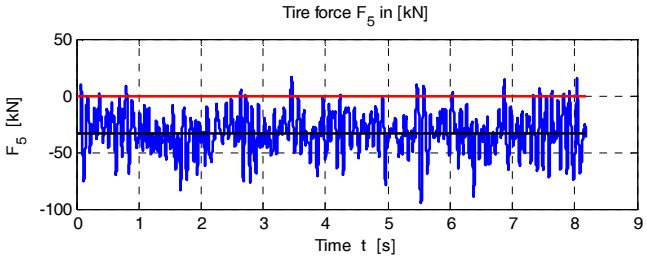

Fig. 20. Tire force under right front wheel, road category E, $S_u(\Omega_0) = 256\cdot10^{-6}$ m^2/(rad/m)

Conclusion

The road unevenness represents the main source of vehicle kinematical excitation. It directly influences the values of the tire forces appearing between the tire and the roadway. It is possible to follow the values of tire forces by in situ experimental tests or by the numerical simulation methods. The present state of computing technique enables the numerical processing of solved problems in real time. At the certain category of the road the tire forces are theoretically plus. In reality the contact between the wheel and the road is lost. The wheel will be bounce from the road. The contact is always replaced by the impact. It is very bad situation for

the pavement straining. So the quality of the road profile is the main factor within the process of the road maintenance.

Acknowledgement

This contribution is the result of the research supported by Grant National Agency VEGA of the Slovak Republic, project No. 1/0295/12.

References

[1] Lajcakova G., Melcer J., Dynamic effect of moving vehicles on the road concrete slabs, Communications 2011, 13, 14-18.

[2] Melcer J. et al., Dynamics of Transport Structure, EDIS, Žilina 2016.

[3] Melcer J. et al., Influence of pavement unevenness on its straining, Civil and Environmental Engineering 2012, 8, 63-77.

[4] Panulinova E., Influence of roar unevenness on the level of noise induced by road transport (in Slovak), Silniční obzor 2001, 62, 275-279.

[5] Kotrasova K., Kormanikova E., Seismic design of liquid storage tank made from composite material, World Journal of Engineering 2008, 5, 445-446.

[6] MATLAB Desktop Tools and Development Environment, Version 7, 2005. The MathWorks, Inc.

[7] ISO 8608, Mechanical vibration - road surface profiles - reporting of measured data, 1995. International standard.

Abstract

The submitted paper is dedicated to the numerical simulation of moving load effect on road structures in the time domain. The dynamic load from vehicles on pavements is the subject of interest. The multi-body computing models of vehicles on various levels are introduces. The equations of motions are derived in the form of ordinary differential equations. The equations of motions are solved numerically by the use of step-by-step integration method in the environment of program system MATLAB. The road unevenness as the main source of kinematical excitation of vehicle is modeled as the random rod profile by the use of the power spectral density functions. The time histories of wonted functions are calculated. Especially the time histories of tire forces as the source of dynamic load of pavements are the object of interest. The conclusions are focused on the influence of the road profile quality on the values of tire forces.

Keywords: Computing models, dynamic load, numerical simulation, pavements, tire forces

Dynamiczne obciążenia nawierzchni - analiza numeryczna

Artykuł poświęcony jest numerycznej symulacji wpływu ruchomego obciążenia na konstrukcje drogowe w dziedzinie czasu. Przedmiotem opracowania są obciążenia dynamiczne nawierzchni od pojazdów. Zaprezentowano wieloetapowe modele obliczeniowe pojazdów na różnych poziomach. Równania ruchu wyprowadzone zostały w postaci równań różniczkowych zwyczajnych. Równania ruchu są rozwiązywane numerycznie za pomocą metody integracji krok po kroku w środowisku systemu programowego MATLAB. Wnioski koncentrują się na wpływie jakości profilu drogi na wartości sił w oponach.

Słowa kluczowe: modele obliczeniowe, obciążenie dynamiczne, symulacja numeryczna, nawierzchnie, siły w oponach